NPhiS2026

NNU·南京师范大学
NANJING NORMAL UNIVERSITY

DM Annihilation with TRIDENT Neutrino Telescope -with Emphasis on $\mathrm{U}(1)_{\mathrm{L_i}-\mathrm{L_j}}$ model

[arXiv: 2601.06817]

Xinhui Chu (褚鑫慧)

Collaboration with Yingwei Wang, Andrew Cheek, Iwan Morton-Blake, Qichao Chang, Samy Kaci, Gwenael Giacinti, Xin Xiang, Donglian Xu, Fuyudi Zhang

May 18, 2026

李政道研究所
TSUNG-DAO LEE INSTITUTE

Content

PART 01

Introduction

WIMP Miracle

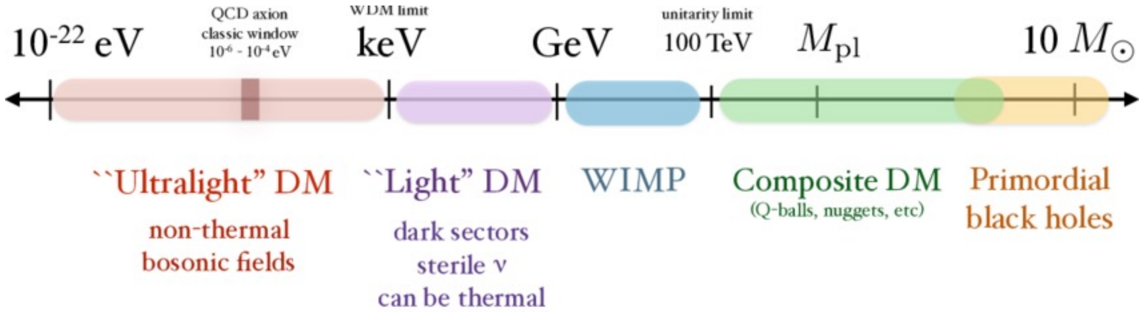

WIMPs: candidates for the dark matter.

If a stable particle with weak-scale interactions exists in the early universe, it would naturally freeze out with a relic abundance.

This process is described quantitatively by the Boltzmann equation:

$$\frac{dn}{dt} + 3Hn = \frac{d(na^3)}{a^3 dt} = \langle\sigma v\rangle \left(n_{eq}^2 - n^2\right)$$

- <σv>: thermally averaged annihilation cross section
- n_{eq}: equilibrium number density $\langle\sigma v\rangle \approx 3\times 10^{-26}\,\mathrm{cm}^3\,\mathrm{s}^{-1}$

[arxiv: 1204.3622]

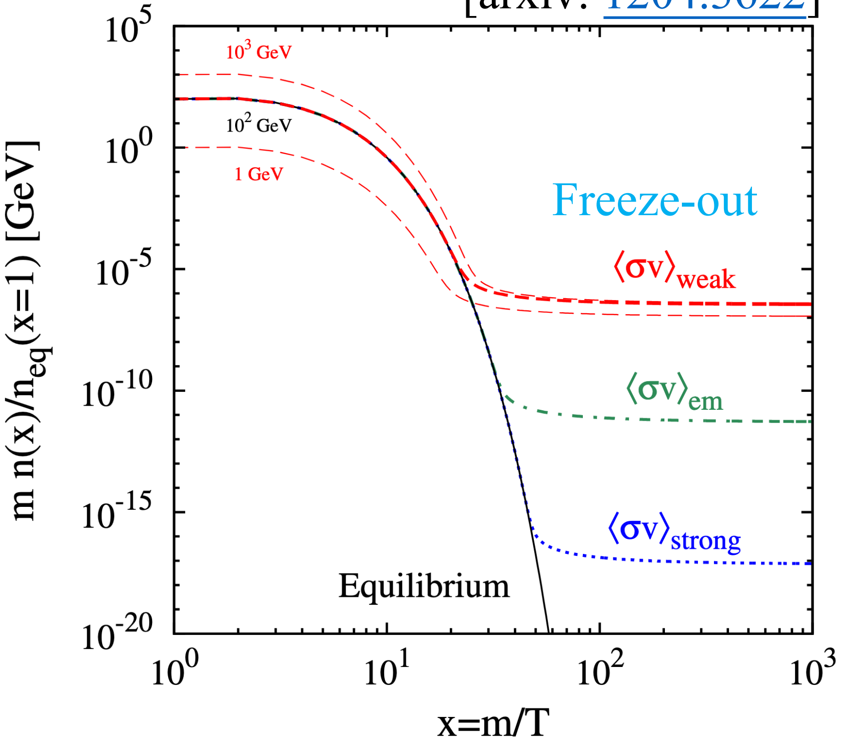

[schumannDirectDetectionWIMP2019]

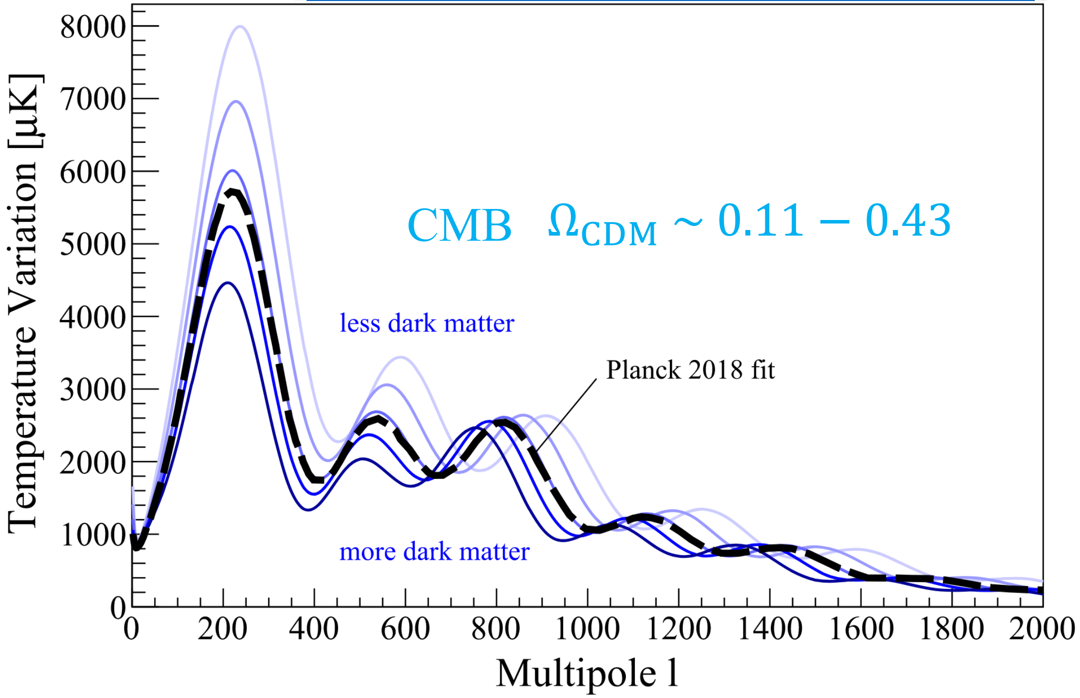

Indirect detection

Annihilation with such a cross-section should in principle be observable in regions of high DM density (like Galactic Centre) , motivating experimental searches.

This method of indirect detection has made substantial progress in the last decades, with the most successful experiments using photons and anti-particles as messengers.

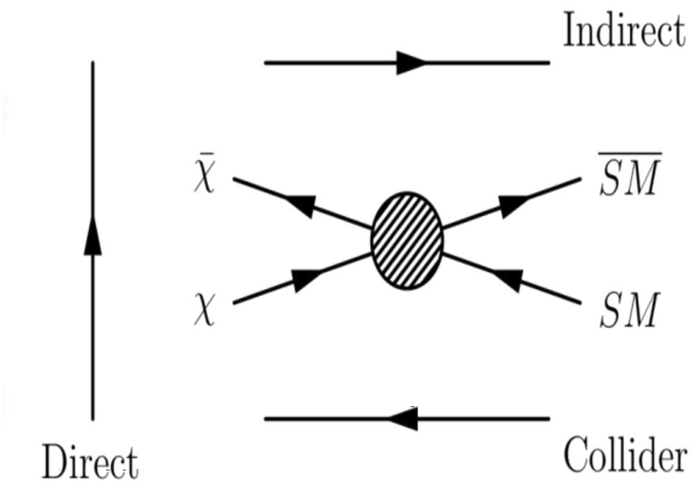

[arxiv: 1805.10305]

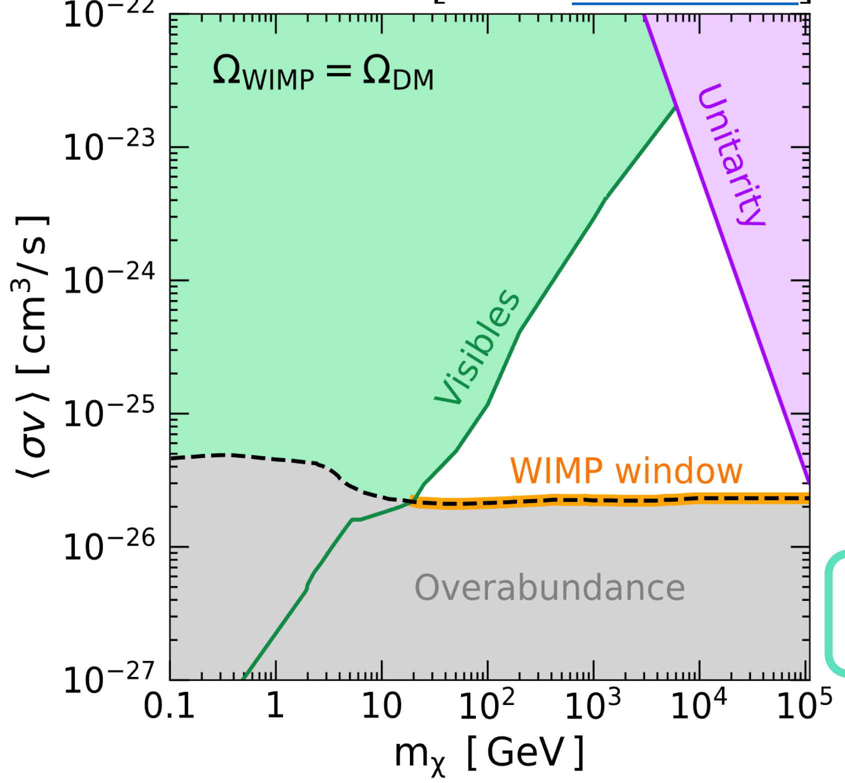

The thermal freeze-out target above ~ 100 GeV remains largely untested!

Indirect

γ-ray telescope

neutrino telescope?

Direct (LZ, PandaX-4T) & Collider detection (ATLAS)

[arxiv: 2404.15930]

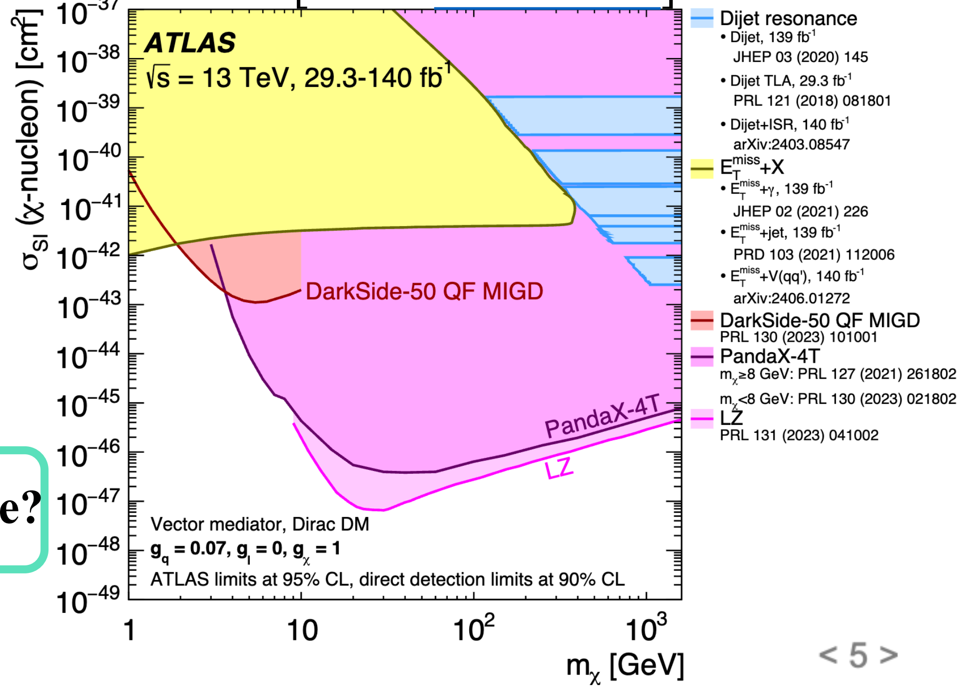

Neutrino telescope

[arxiv: 1912.09486]

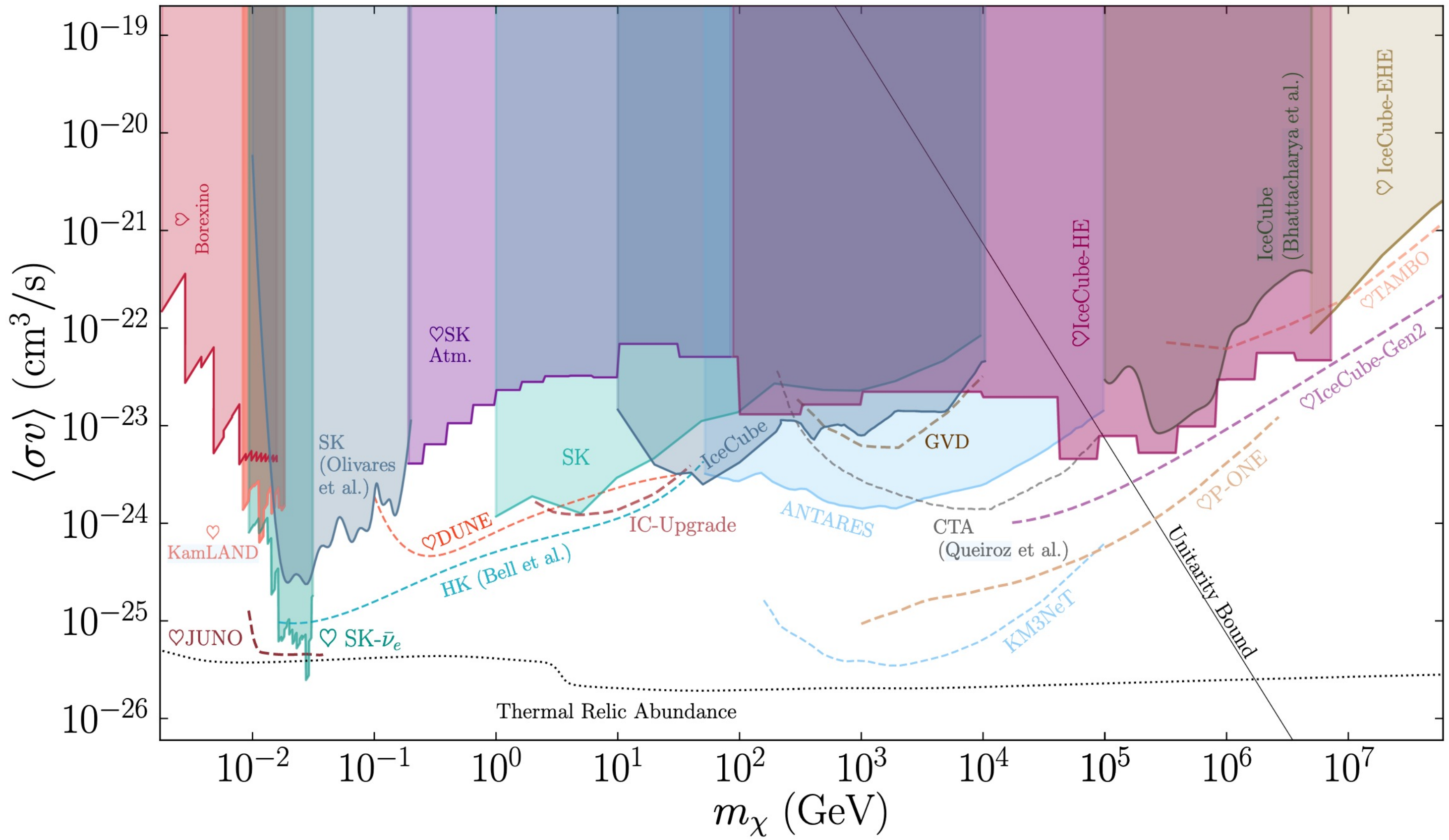

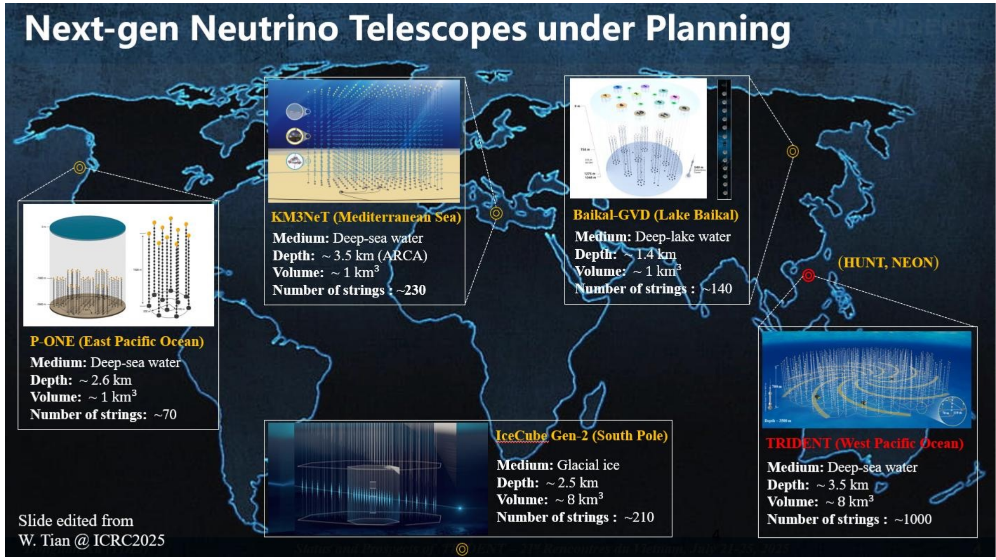

TRIDENT: in the search for DM in the $10^3 - 10^5$ GeV mass range

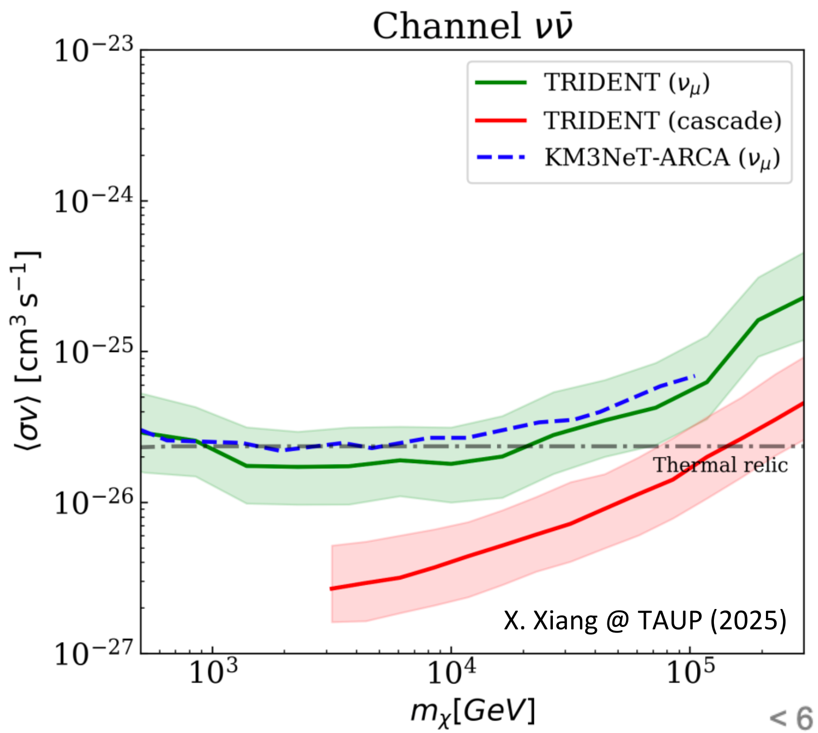

Currently neutrino telescopes are far from the relic line (except below ~ 1GeV).

KM3NeT stands a chance to make big gains.

TRIDENT will be roughly 10 times as big as KM3NeT!

PART 02

TRIDENT Sensitivity

TRIDENT Detector

$$\chi\,\chi \longrightarrow \nu\,\bar{\nu}\,\gamma\,e\,\tau\,b\,\ldots$$

$$\boxed{\frac{d\Phi_\nu}{dE_\nu}} = \frac{1}{4\pi}\frac{\langle\sigma v\rangle}{\kappa m_\chi^2}\left(\sum_\alpha \boxed{\frac{dN^{\mathrm{prod}}_{\nu\alpha}}{dE_{\nu\alpha}}}\,\boxed{P_{\nu\alpha\to\nu\beta}}\right)\boxed{J(\Omega)} \rightarrow$$

J-factor describes the astrophysical dependence of the DM signal

The expected neutrino flux from DM annihilation

The neutrino energy spectrum per DM annihilation

The transition probability from the source to detector

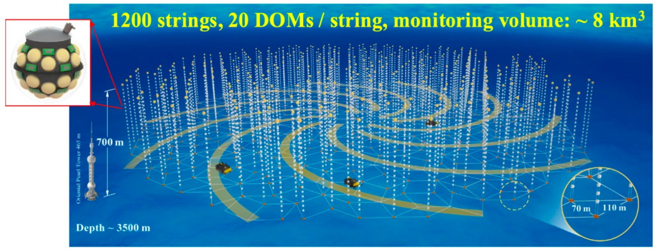

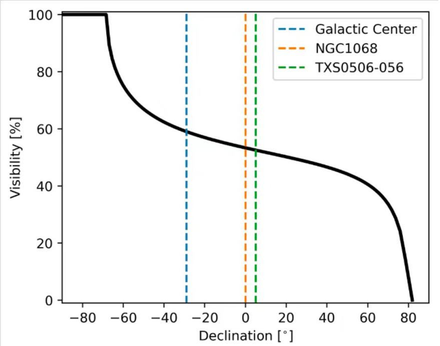

Visibility of TRIDENT (Fuyudi Zhang)

TRIDENT detector response

- Large volume ⟶ large effective area
- Equatorial location ⟶ full-sky coverage
- Water-based ⟶ better angular resolution

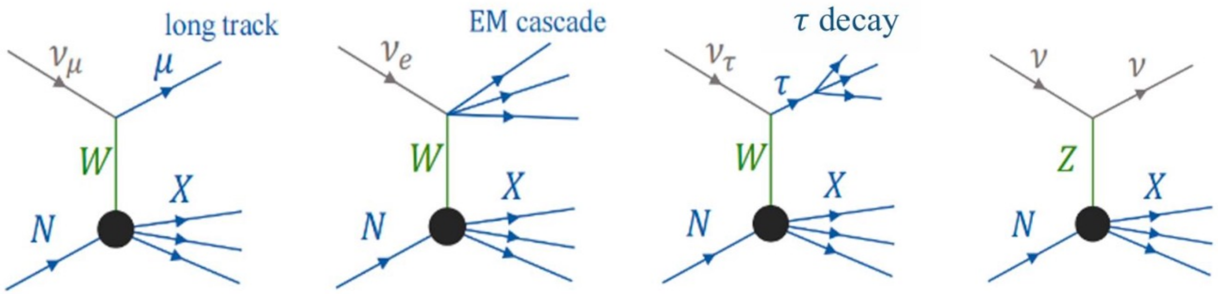

Neutrino interactions in TRIDENT produce two main event topologies: tracks and cascades

Tracks ⟶ providing the best direction information

Cascades ⟶ better energy resolution and lower atmospheric background

Standard Sensitivity

We forecast the sensitivity of TRIDENT to DM annihilation into some specific SM final states, assuming a 100% branching ratio for each channel.

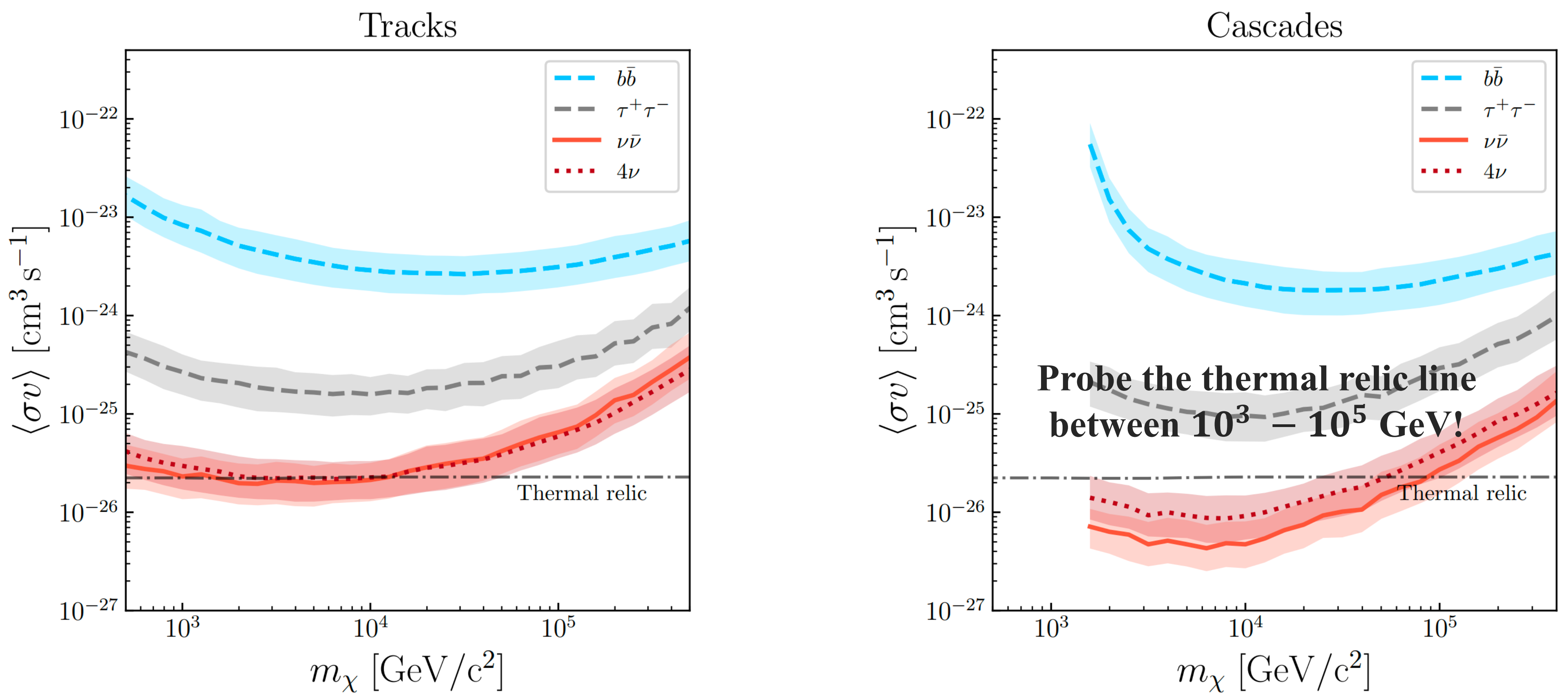

We shows the 95% CL upper limits for the $b\bar{b}$, $\tau^+\tau^-$, $\nu\bar{\nu}$ and 4ν channels obtained from the maximum-likelihood analysis. The lines represent the median expected limits, while the colour bands denote the 68% intervals around the expected value, taking into account the statistical uncertainties from Monte Carlo simulations.

Galactic Plane Background and the Halo Uncertainty

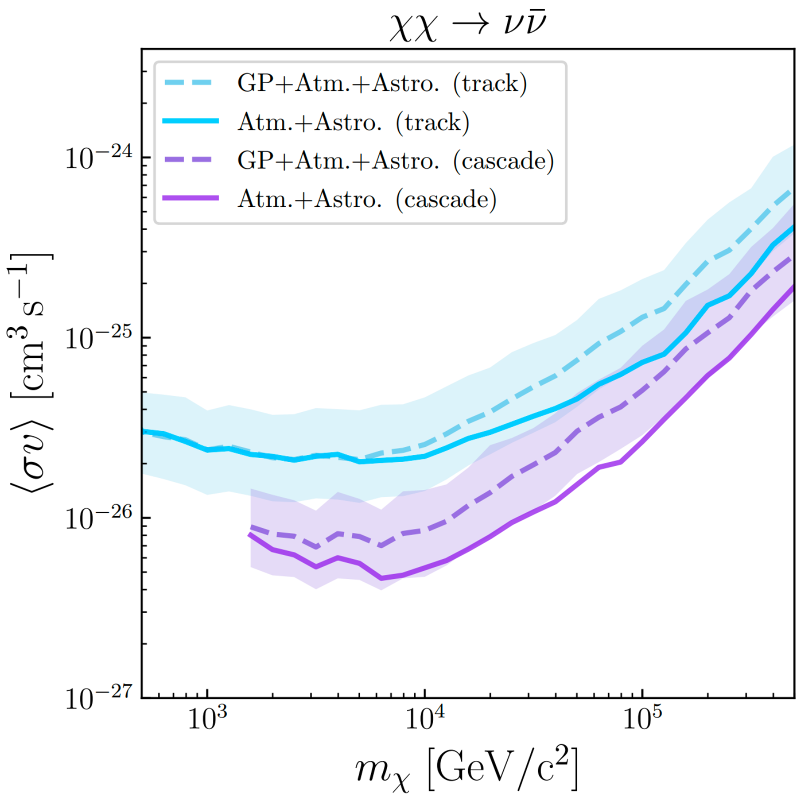

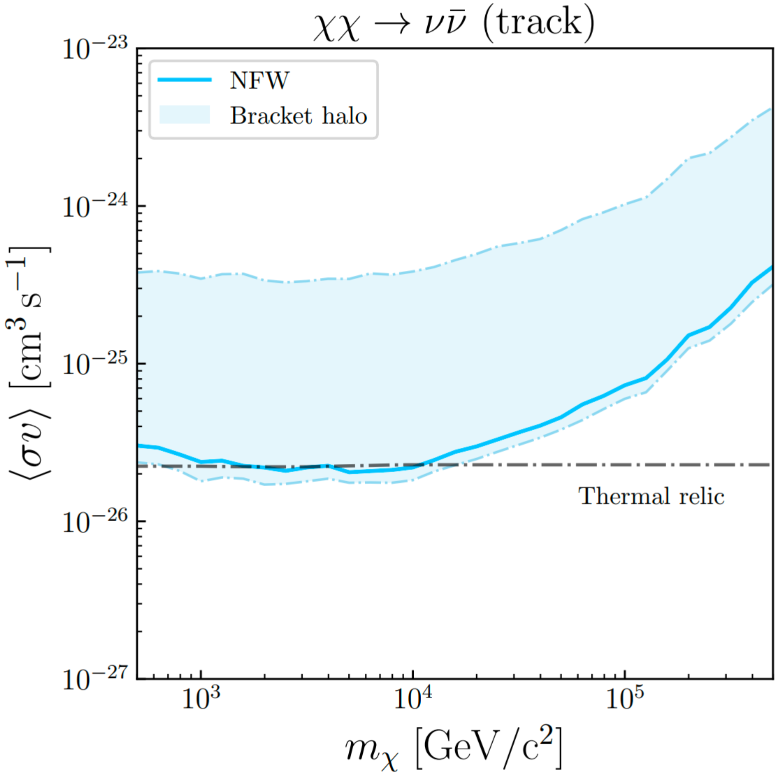

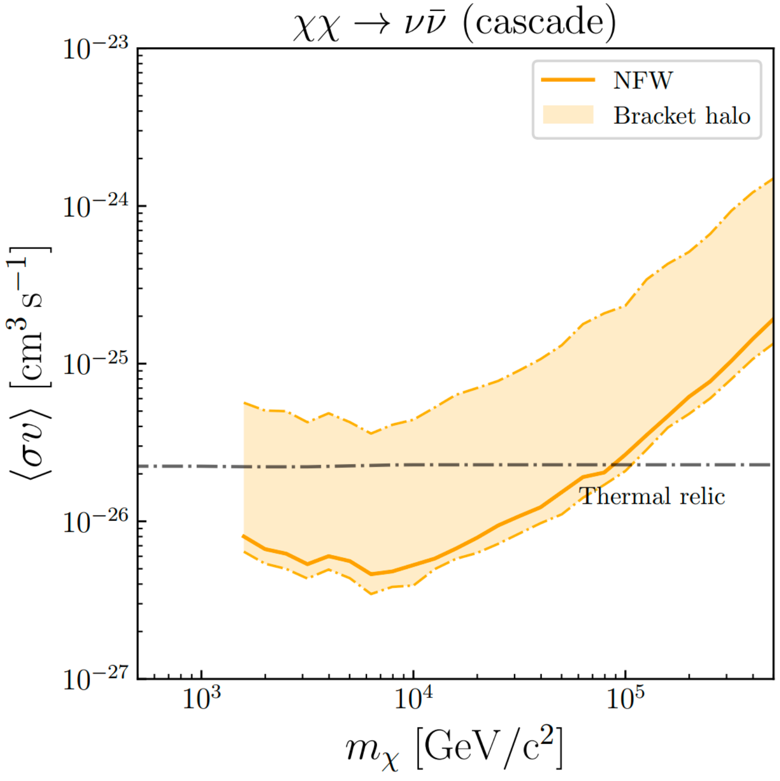

Galactic Plane Background

The effect dominated in the high-energy region. The cascade events are more affected due to the limited angular resolution.

The Halo Uncertainty

The bracket Milky way dark matter halo model from arXiv:2501.14868 used series of simulations in the conditions of adiabatically contracted or strong baryonic feedback, consistent with observed stellar distribution.

PART 03

Constraints on $U(1)_{L_i - L_j}$ model

$\mathrm{U(1)_{L_i-L_j}}$ model

The $\mathrm{U(1)_{L_i-L_j}}$ extension of the SM is one of the simplest theoretically consistent extensions available. There is the new $\mathrm{U(1)_{L_i-L_j}}$ boson, Z′, which couples to the SM via the following current

$$j_\alpha^{L_i-L_j} = \bar{L}_i\gamma_\alpha L_i + \bar{\ell}_i\gamma_\alpha \ell_i - \bar{L}_j\gamma_\alpha L_j - \bar{\ell}_j\gamma_\alpha \ell_j.$$

$\mathrm{U(1)_{L_\mu-L_\tau}}$

$\mathrm{U(1)_{L_e-L_\mu}}$

$\mathrm{U(1)_{L_e-L_\tau}}$

The dark sector is then

$$j_\alpha^\chi = \bar{\chi}\gamma_\alpha\chi = \bar{\chi}_L\gamma_\alpha\chi_L + \bar{\chi}_R\gamma_\alpha\chi_R$$

such that the interaction terms are

$$\mathcal{L}_{\text{int}} = \frac{\epsilon}{2\cos\theta_W} B_{\alpha\beta}Z'^{\alpha\beta} + g_{Z'}^{\mathrm{DM}} Z'^{\alpha} j_\alpha^\chi + g_{Z'}^{\mathrm{SM}} Z'^{\alpha} j_\alpha^{L_i-L_j}$$

$$\boxed{\epsilon(p\to 0) = \frac{e\, g_{Z'}^{\mathrm{SM}}}{6\pi^2}\ln\left(\frac{m_j}{m_i}\right)}$$

At tree-level, DM annihilation channels could be $\chi\bar{\chi} \to \tau\bar{\tau}$, $\chi\bar{\chi} \to \mu\bar{\mu}$, $\chi\bar{\chi} \to \nu_\tau\bar{\nu_\tau}$, $\chi\bar{\chi} \to \nu_\mu\bar{\nu_\mu}$, $\chi\chi \to Z'Z'$.

s-channel

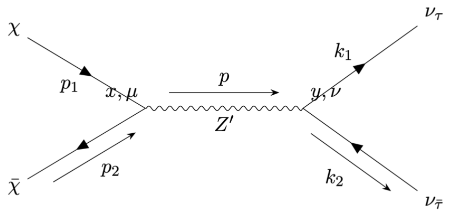

t-channel

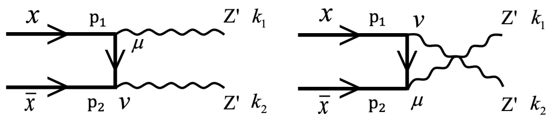

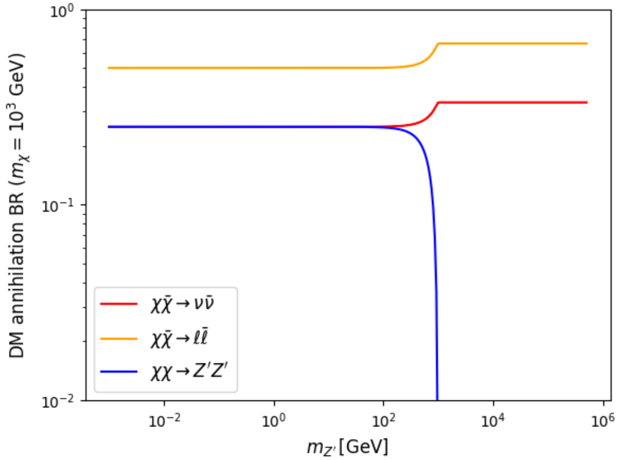

For light mediator , the branching ratio of process $\chi\chi \to Z'Z'$ is $\mathrm{Br}_{Z'Z'} = 0.25$.

For heavy mediator,

$$\langle\sigma v\rangle_{\chi\chi\to\nu\bar{\nu}} = \frac{1}{2}\langle\sigma v\rangle_{\chi\chi\to\ell^+\ell^-} = \frac{1}{3}\langle\sigma v\rangle_{\text{tot}}.$$

$\mathrm{U(1)}_{\mathrm{L_i-L_j}}$ model

The current constraints on the $\mathrm{U(1)}_{\mathrm{L_\mu-L_\tau}}$ model is

[arxiv: 2603.19467]

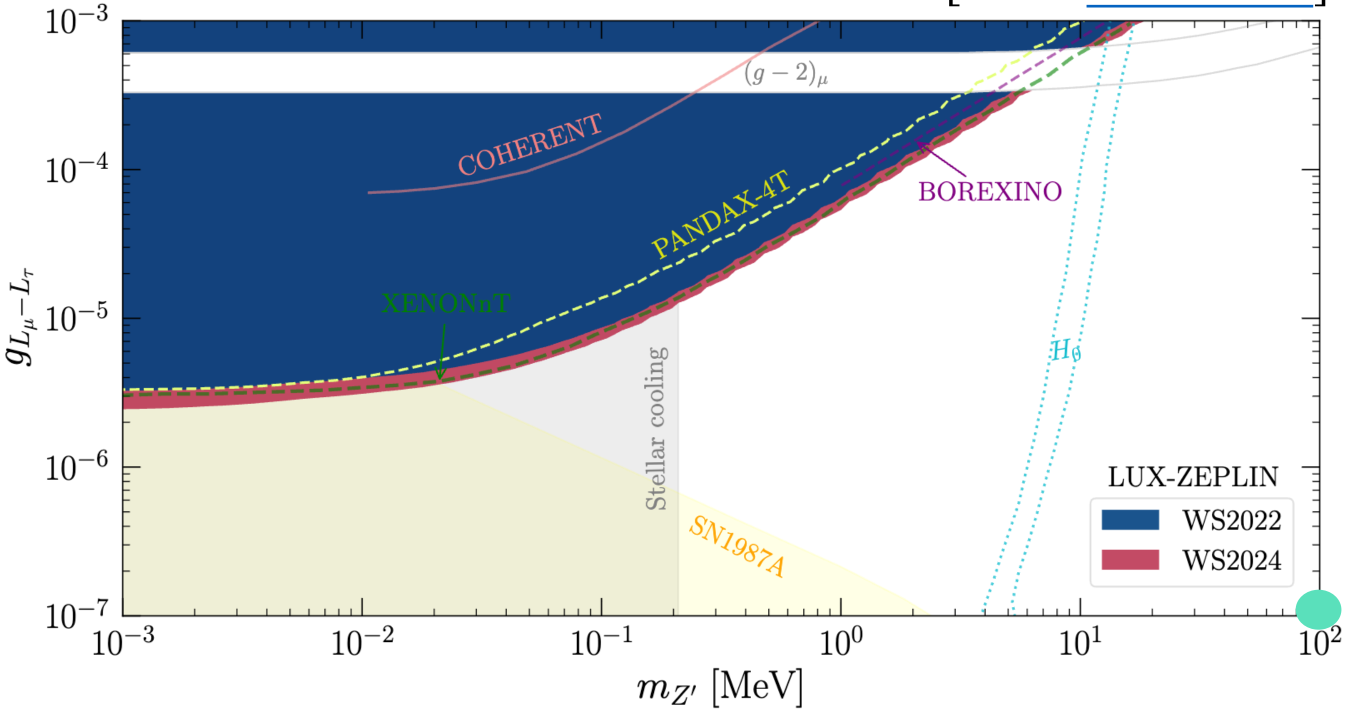

[M.-W. Li, X.-G. H, A. C, **XC**]

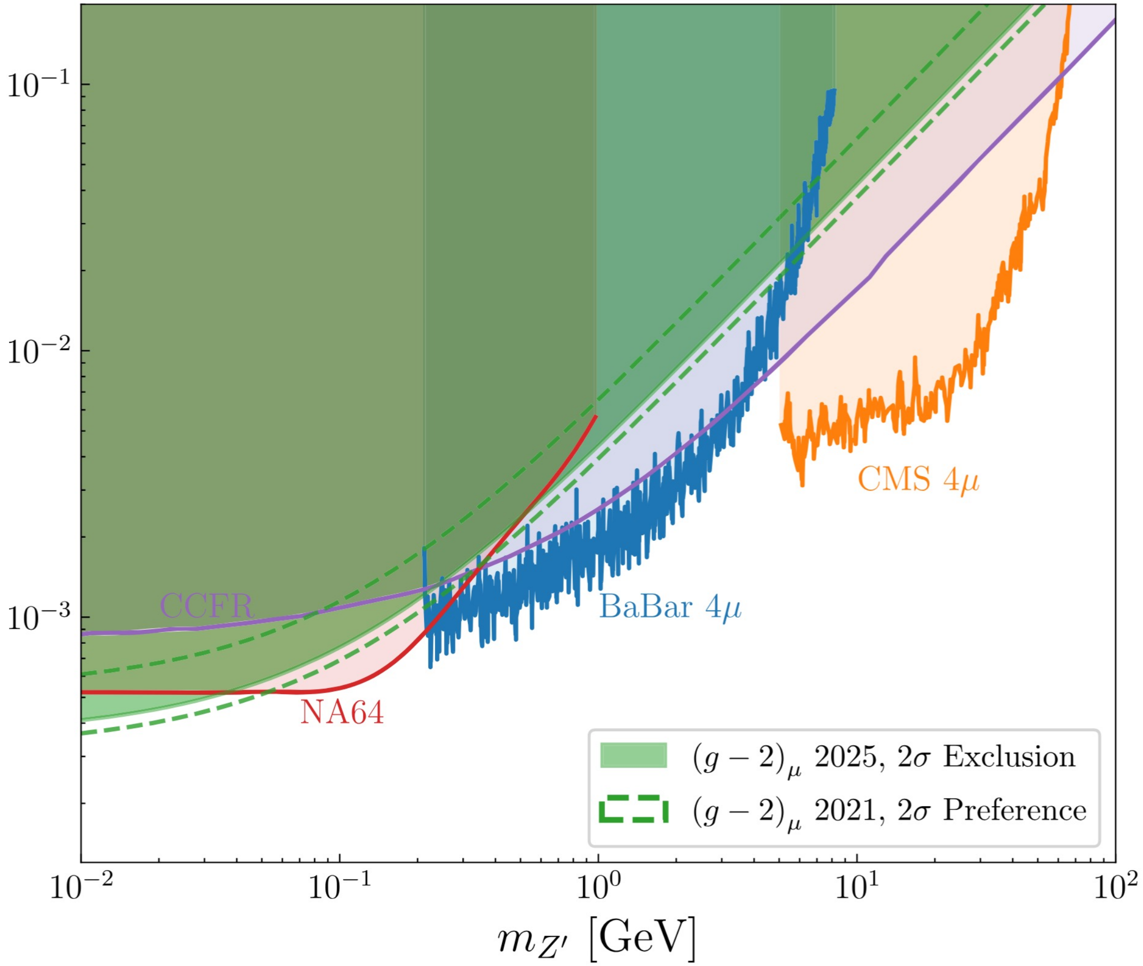

Explore large mass regions of the new gauge boson Z' !

The thermal relic line

First, when calculating the thermally averaged cross-section during thermal freeze-out we use

$$\langle \sigma v \rangle = \frac{2\pi^2 T}{\left(4\pi m_\chi^2 T K_2(m_\chi/T)\right)^2} \int_{4m_\chi}^{\infty} ds \sqrt{s}(s - 4m_\chi^2) K_1\left(\frac{\sqrt{s}}{T}\right) \sigma_{\chi\chi\to ff}(s)$$

assuming the Maxwell-Boltzmann distribution of the DM phase space.

[arxiv: 1204.3622]

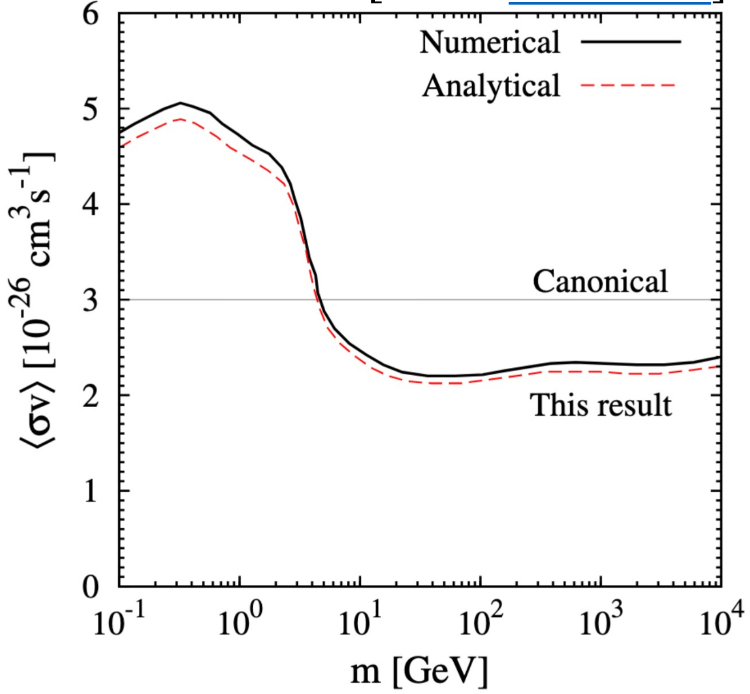

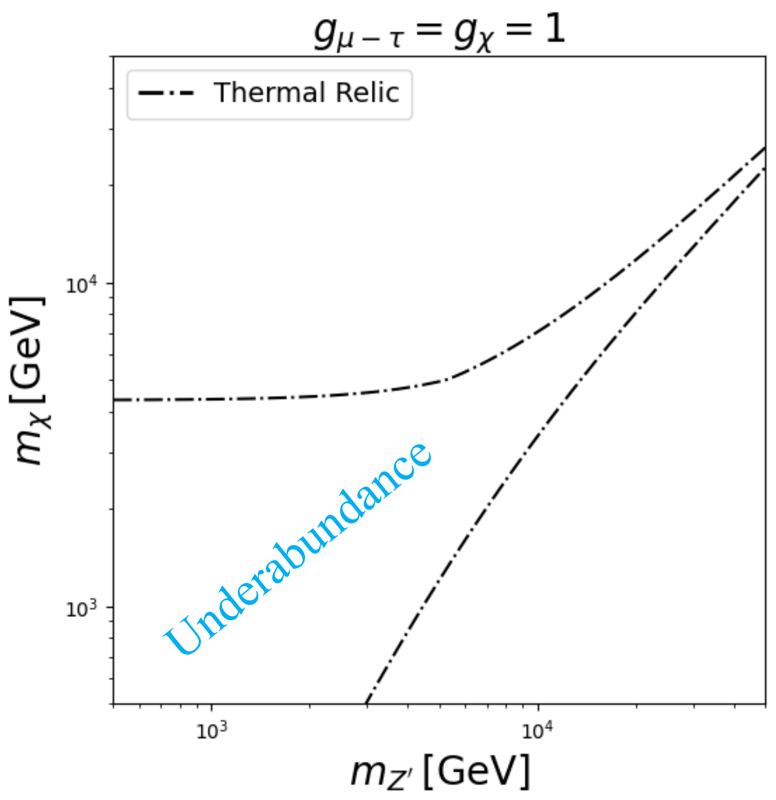

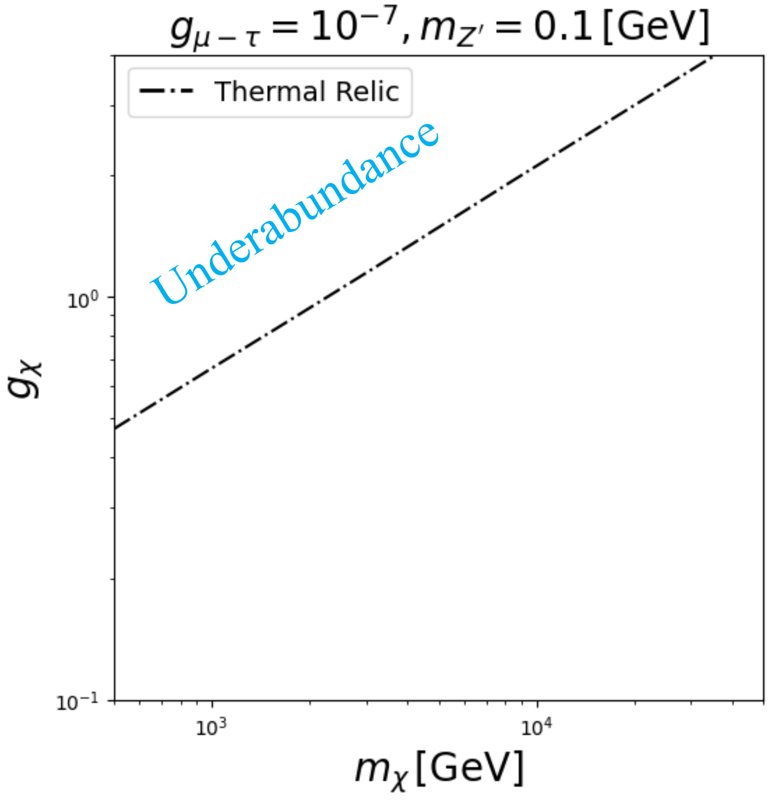

The constraints from TRIDENT

Although the dynamics of the early universe and now is the same, the kinematics are largely different. We replace the phase distribution to velocity distribution,

$$\langle \sigma v \rangle_i = \int \mathrm{d}v_{\rm rel}\, \tilde{f}_{\rm rel}(v_{\rm rel})\, \sigma_i v_{\rm rel}$$

assuming the Maxwell-Boltzmann distribution of DM velocity.

For s-channel, Sommerfeld Enhancement

$$\sigma v = S\,(\sigma v)_0$$

$$S(v) \propto \frac{1}{v^2}\text{, resonances}$$

$$S(v) \propto \frac{1}{v}\text{, away from resonances}$$

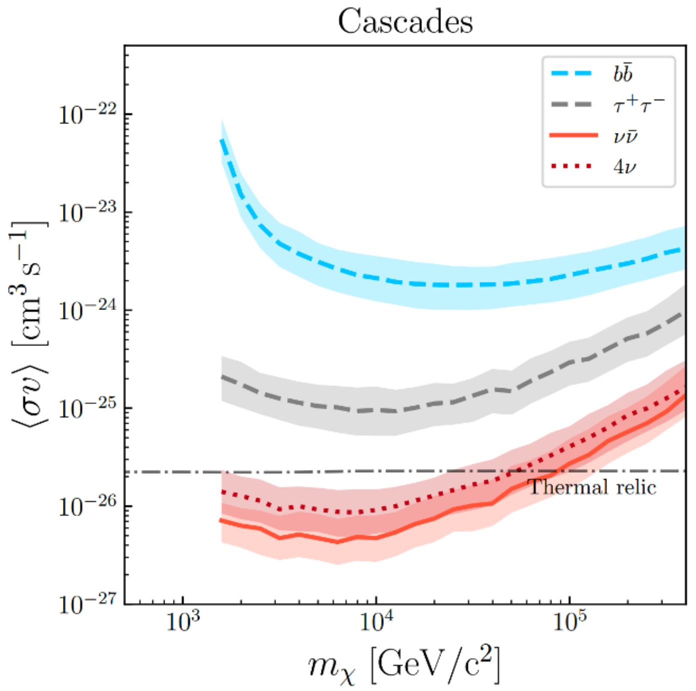

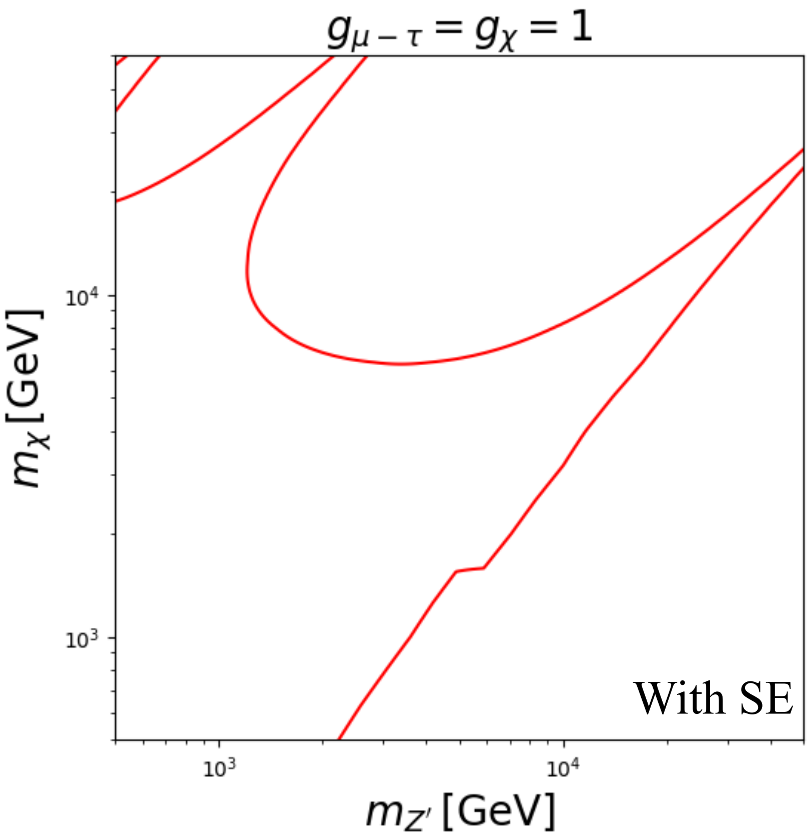

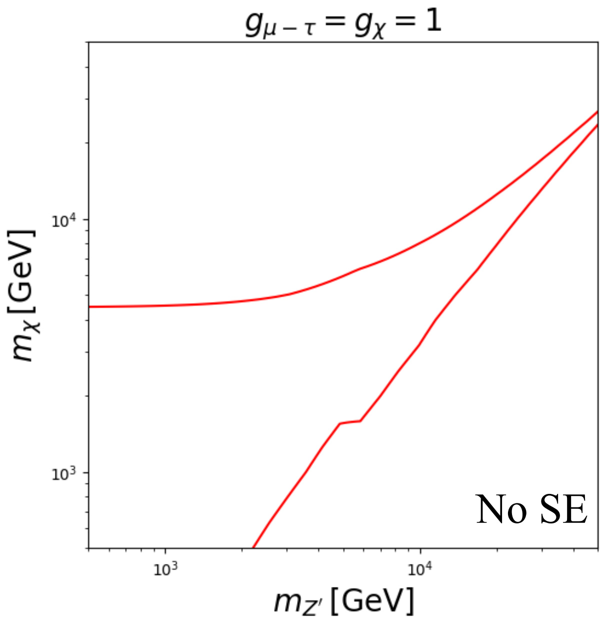

The constraints from TRIDENT

When the mediator Z' is lighter than DM, the box-shaped spectra via the decay of Z' after the annihilation $\chi\chi \to Z'Z'$ is considerable. For such channels we determine the branching ratio by (multiply by 2 if $i \neq j$).

$$\mathrm{Br}_{i\bar{i}\,j\bar{j}} = \mathrm{Br}_{Z'Z'} \times \left(\frac{\Gamma\left(Z' \to i\bar{i}\right)}{\Gamma_{\mathrm{tot}}}\right) \times \left(\frac{\Gamma\left(Z' \to j\bar{j}\right)}{\Gamma_{\mathrm{tot}}}\right)$$

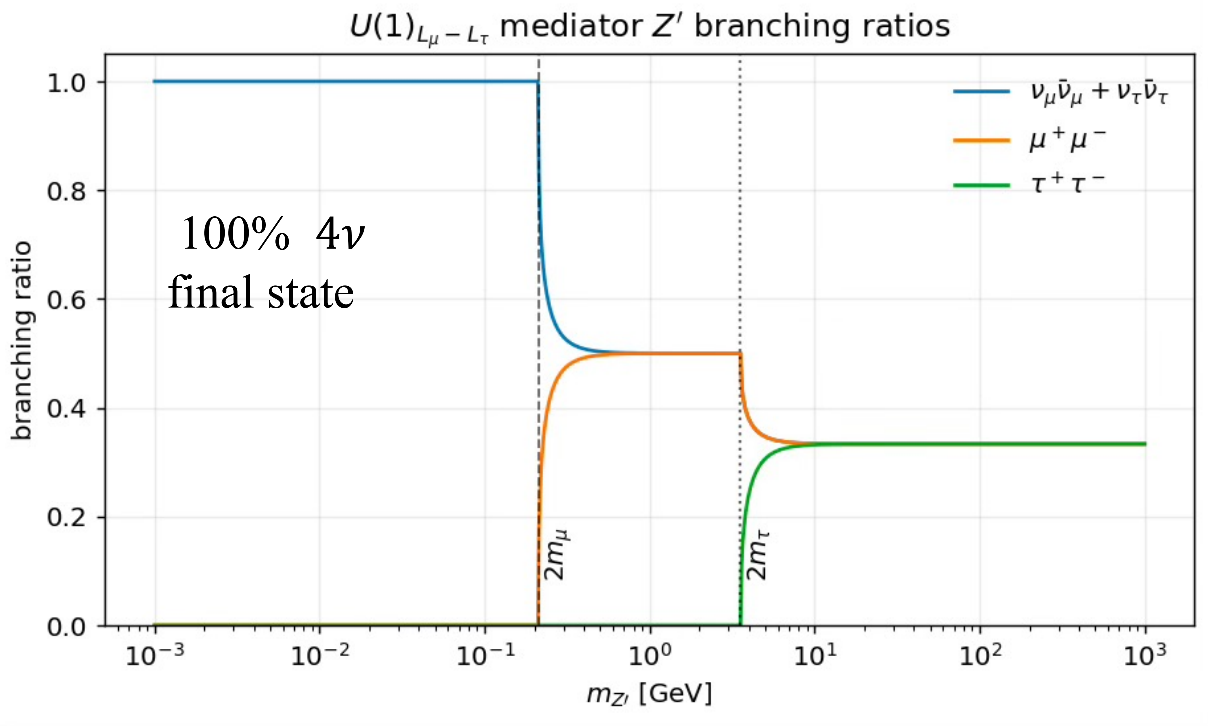

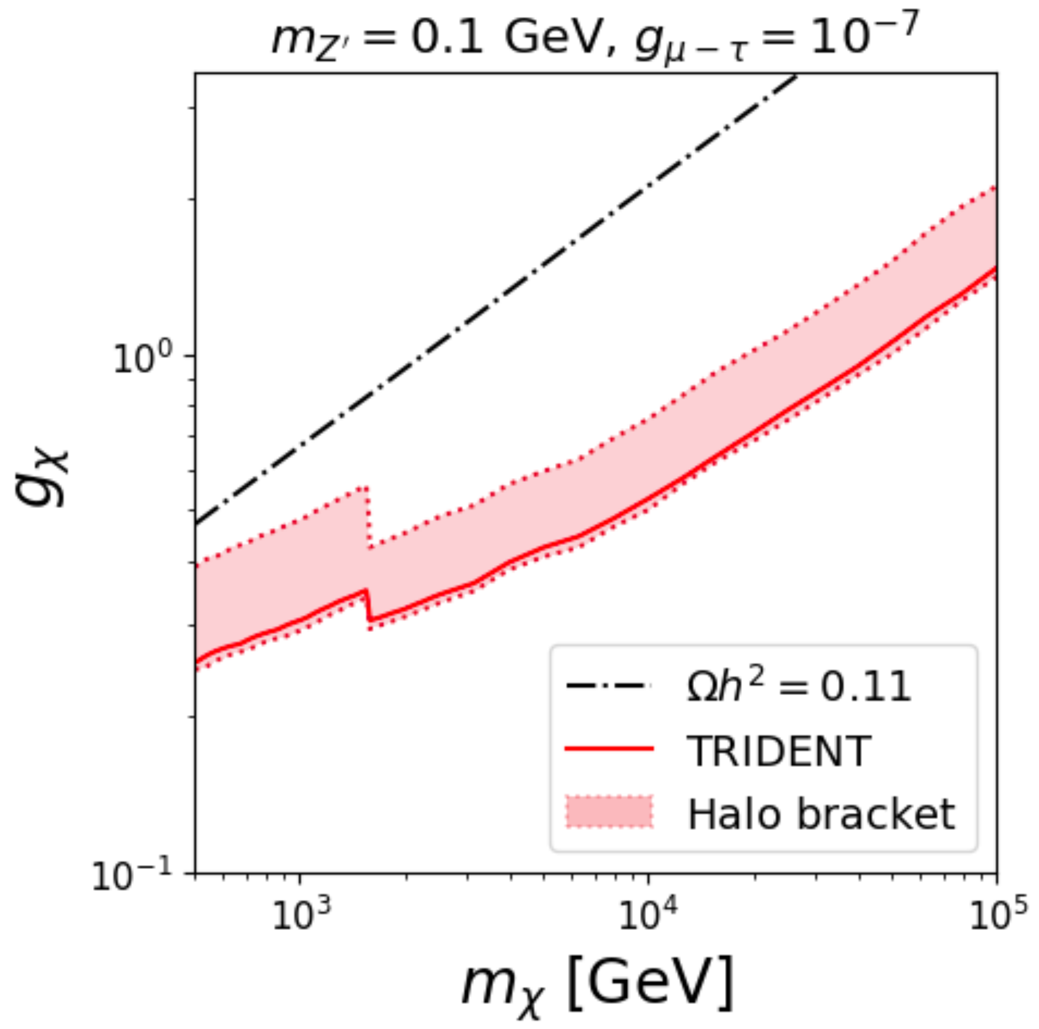

The solid red line is for the NFW profile and the red shaded region brackets the uncertainty in the halo, we see when $m_\chi \gtrsim 600$ GeV, TRIDENT's sensitivities will be able to confidently exclude this scenario for thermally produced DM.

The constraints from Pandax-4T

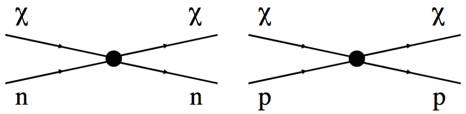

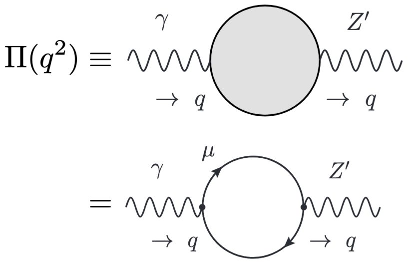

$$\boxed{\Pi_2(0) = \frac{e g_{\mu-\tau}}{12\pi^2} \ln \frac{m_\tau^2}{m_\mu^2}}$$

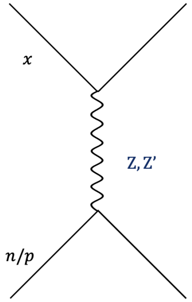

$$\mathcal{L}_{int} = -g_1 j_\mu^Y \hat{B}^\mu - g_2 j_\mu^3 \hat{W}^{3\mu} - g_x j_\mu^x \hat{X}^\mu,$$

$$\mathcal{L}_{int}^A = -A^\mu g_2 \sin\theta_w j_\mu^{EM},$$

$$\begin{pmatrix} \hat{B}_\mu \\ \hat{W}_\mu^3 \\ \hat{X}_\mu \end{pmatrix} = G(\epsilon_Y) S^T \begin{pmatrix} A_\mu \\ Z_\mu \\ Z'_\mu \end{pmatrix}.$$

$$\mathcal{L}_{int}^Z = -Z^\mu g_x j_\mu^x \sin\xi - Z^\mu \frac{g_2}{\cos\theta_w}(-j_\mu^Y \epsilon_Y \sin\theta_w \sin\xi + j_\mu^Z \cos\theta_w \cos\xi),$$

$$\mathcal{L}_{int}^{Z'} = -Z'^\mu g_x j_\mu^x \cos\xi - Z'^\mu \frac{g_2}{\cos\theta_w}(-j_\mu^Y \epsilon_Y \sin\theta_w \cos\xi - j_\mu^Z \cos\theta_w \sin\xi).$$

$$\tan(\xi) = \frac{\epsilon_Y \sin\theta_w m_Z^2}{m_Z^2 - m_{Z'}^2} = \frac{e g_{\mu-\tau} \tan\theta_w m_Z^2}{12\pi^2 (m_Z^2 - m_{Z'}^2)} \ln \frac{m_\tau^2}{m_\mu^2}$$

$\tan\xi$ is quite small for both light mediator and heavy mediator. When $m_{Z'} > 2\mu_{\chi N}\, v_\chi \sim 0.1$ GeV, then we could say

$$\mathcal{M} \propto -\frac{g_2 g_\chi \sin\theta_w \cos\theta_w \epsilon_Y}{m_{Z'}^2}(Y + T^3)$$

$$\sigma_{\chi p} = \frac{\overline{|\mathcal{M}|^2}}{16\pi s} = \frac{m_\chi^2 m_p^2}{\pi(m_\chi + m_p)^2} \frac{g_2^2 g_\chi^2 \sin^2\theta_w \cos^2\theta_w \epsilon_Y^2}{m_{Z'}^4}.$$

$$\sigma_{\chi p} = \sum_i p_i \left(\frac{A_i}{Z}\right)^2 \sigma_{\chi n}^{\exp}$$

p_i is the abundance of different isotopes.

The constraints from Pandax-4T

[arxiv: 2408.00664]

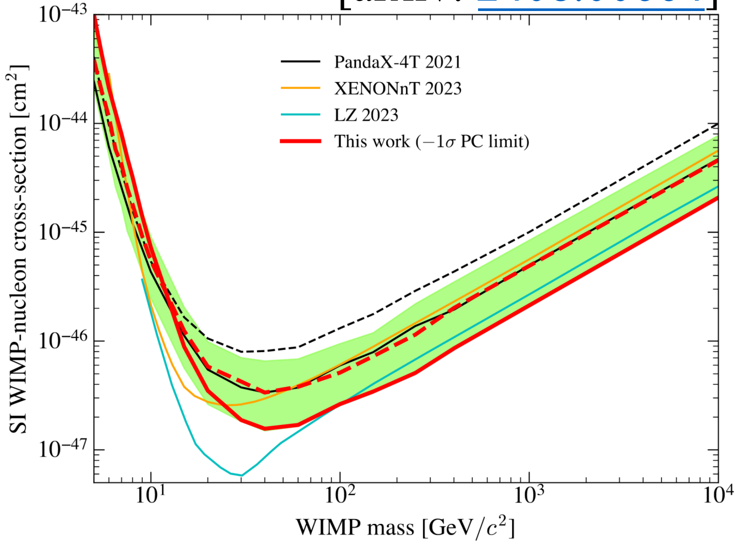

[arxiv: 2109.03116]

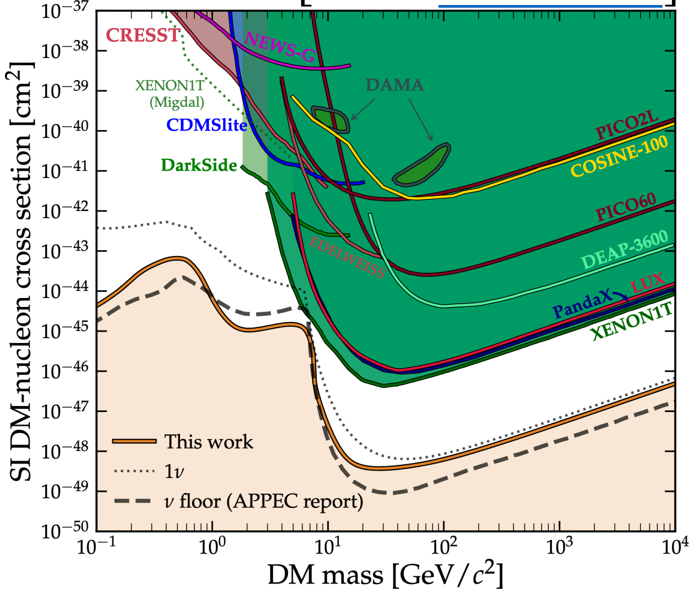

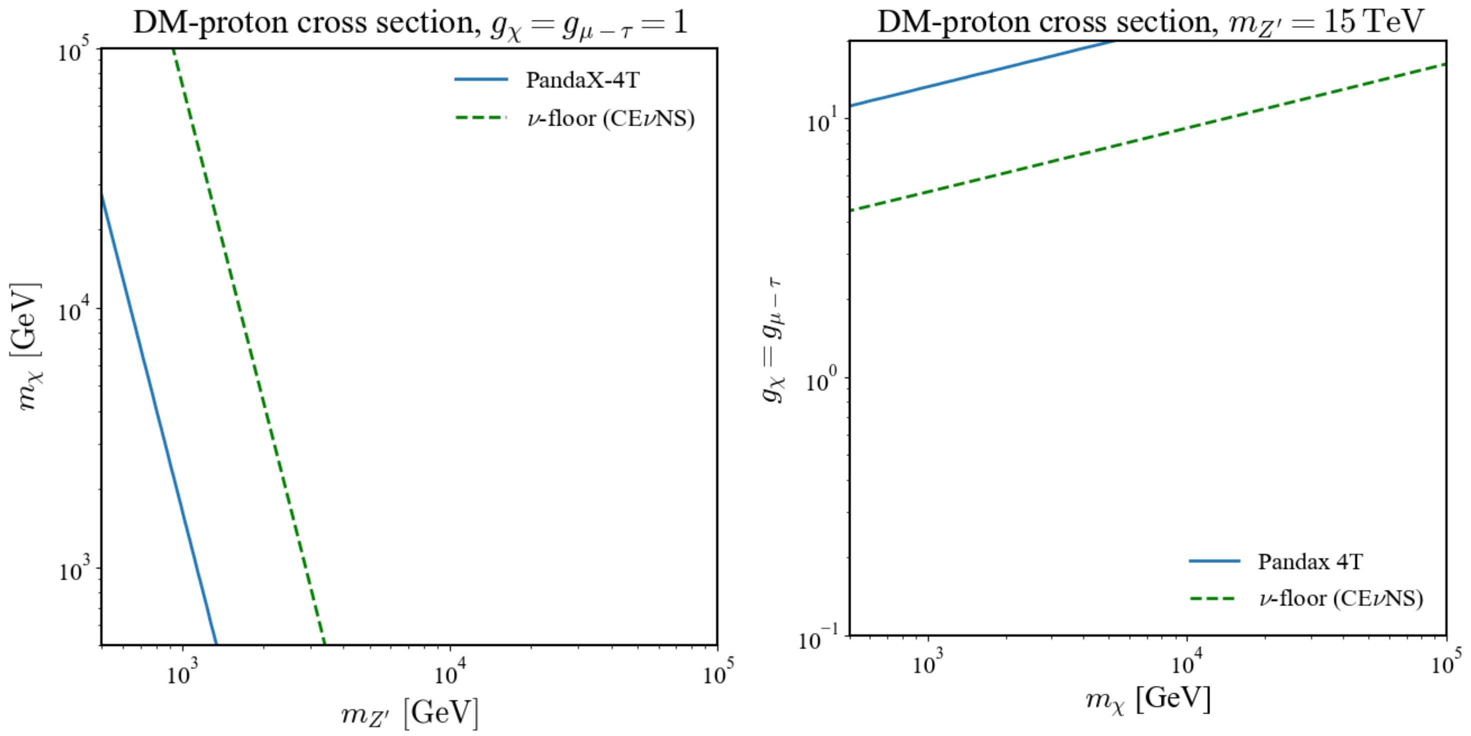

In the left panel, the left region of blue line where the cross section exceeds the upper limit of PandaX-4T could be excluded and the right region is what we could explore in other DM detections. The green dashed line gives the limit of ν −floor, and the right region is where DM signals couldn't be distinguished from neutrino background.

The same type of signal can also be induced by coherent elastic neutrino-nucleus scattering (CEνNS) from solar, atmospheric, and diffuse supernova neutrinos.

PART 04

Conclusion

Conclusion

The first DM annihilation sensitivity forecasts for TRIDENT

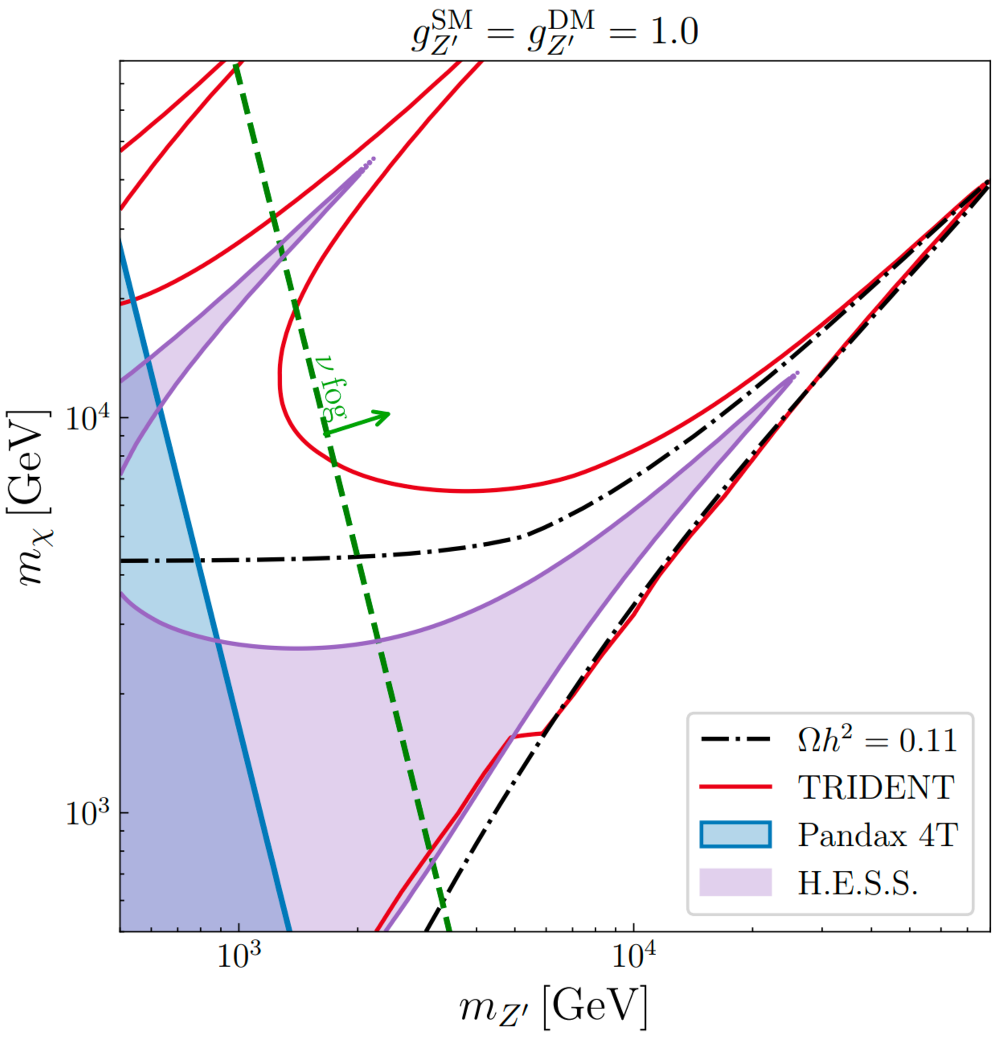

$U(1)_{L_i - L_j}$ model:
Show that TRIDENT can outperform γ-ray telescopes and direct detection experiments in certain parameter regions.

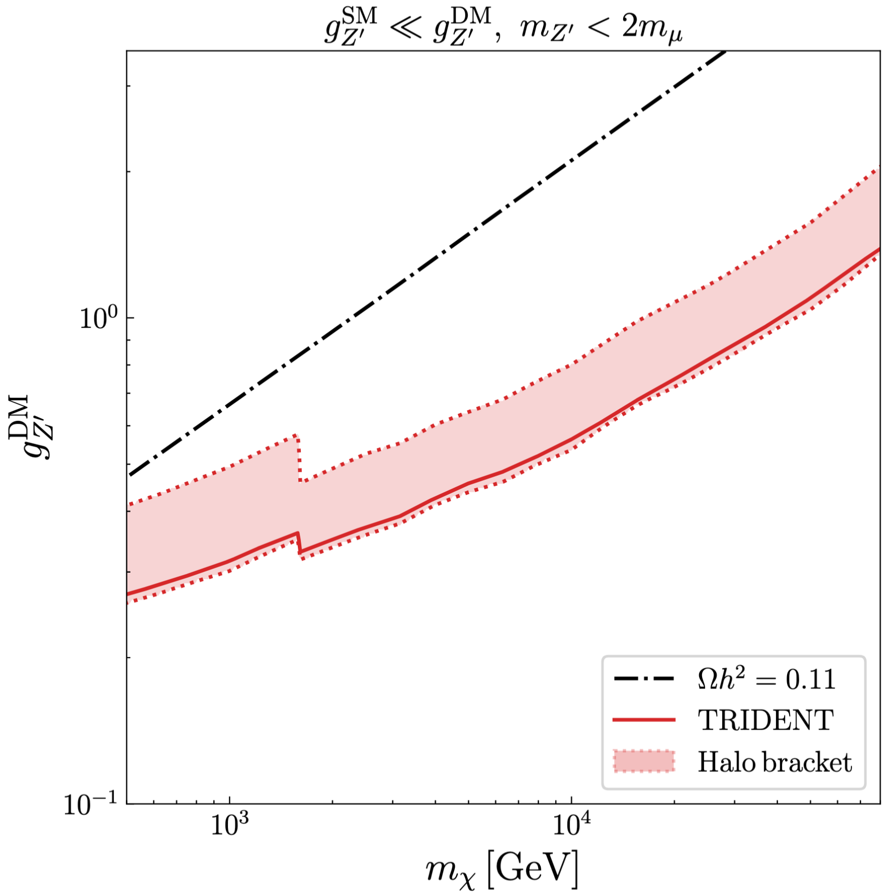

NNU · 南京师范大学
NANJING NORMAL UNIVERSITY

Thank you for attention!

李政道研究所
TSUNG-DAO LEE INSTITUTE

Back up

Model-independent Limits

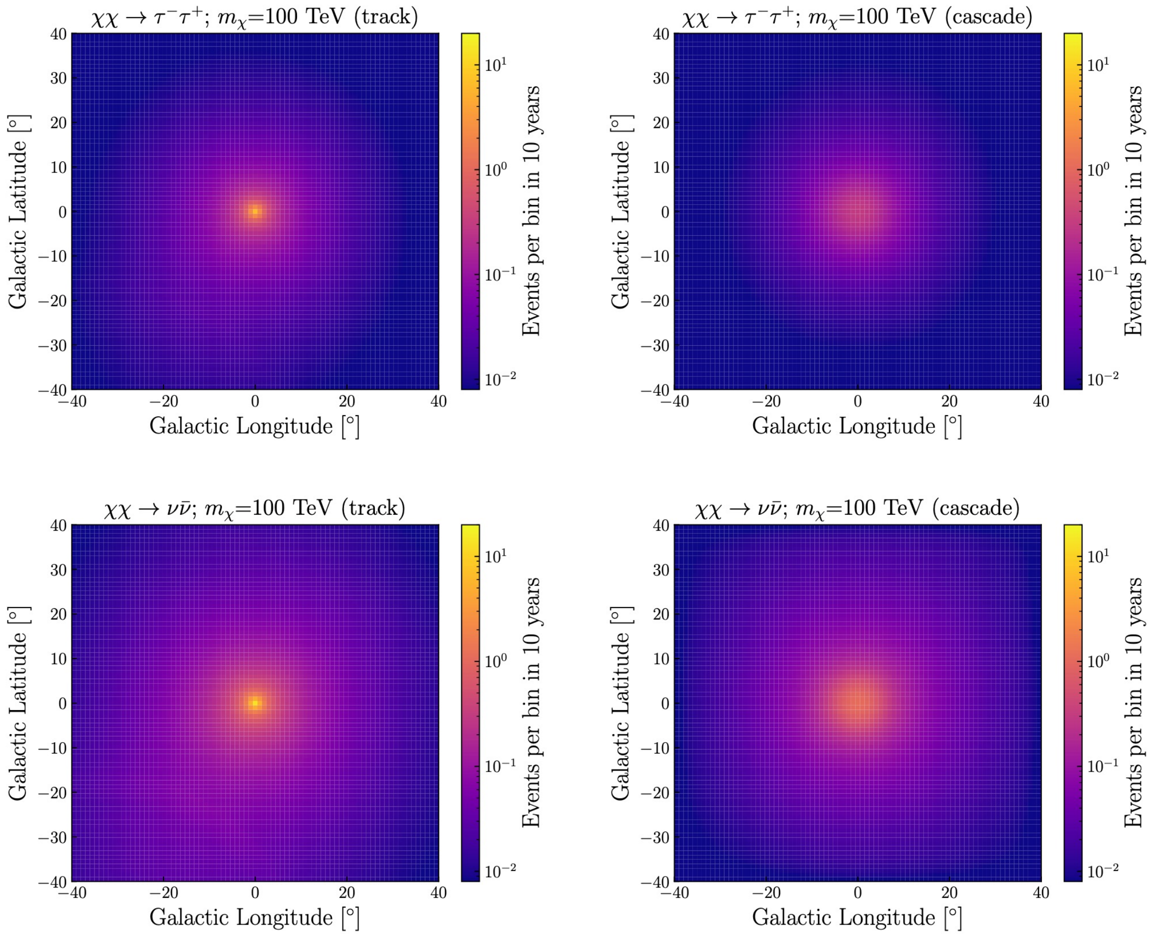

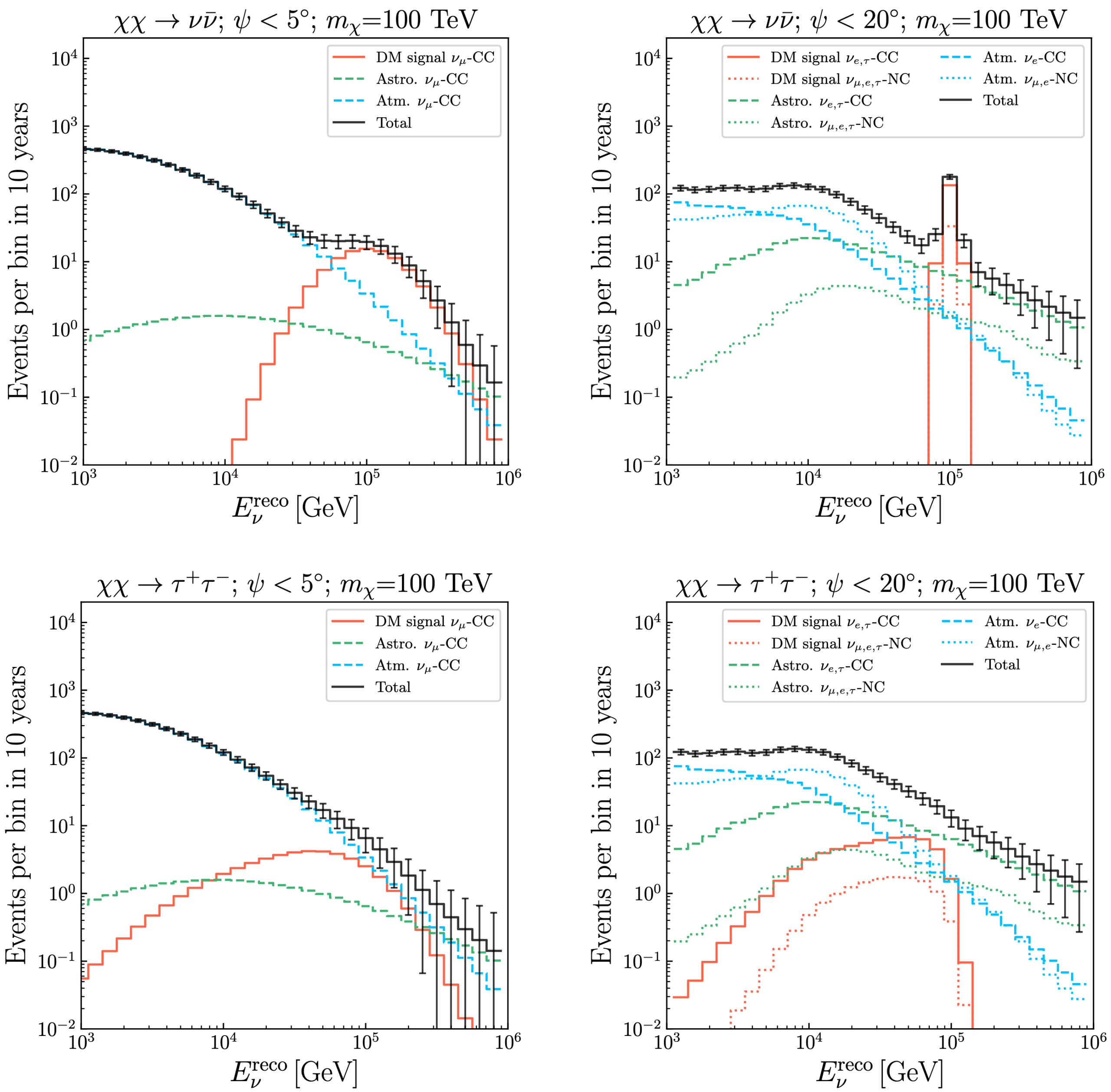

The other cases

$U(1)_{L_e - L_\mu}$?

$U(1)_{L_e - L_\tau}$?

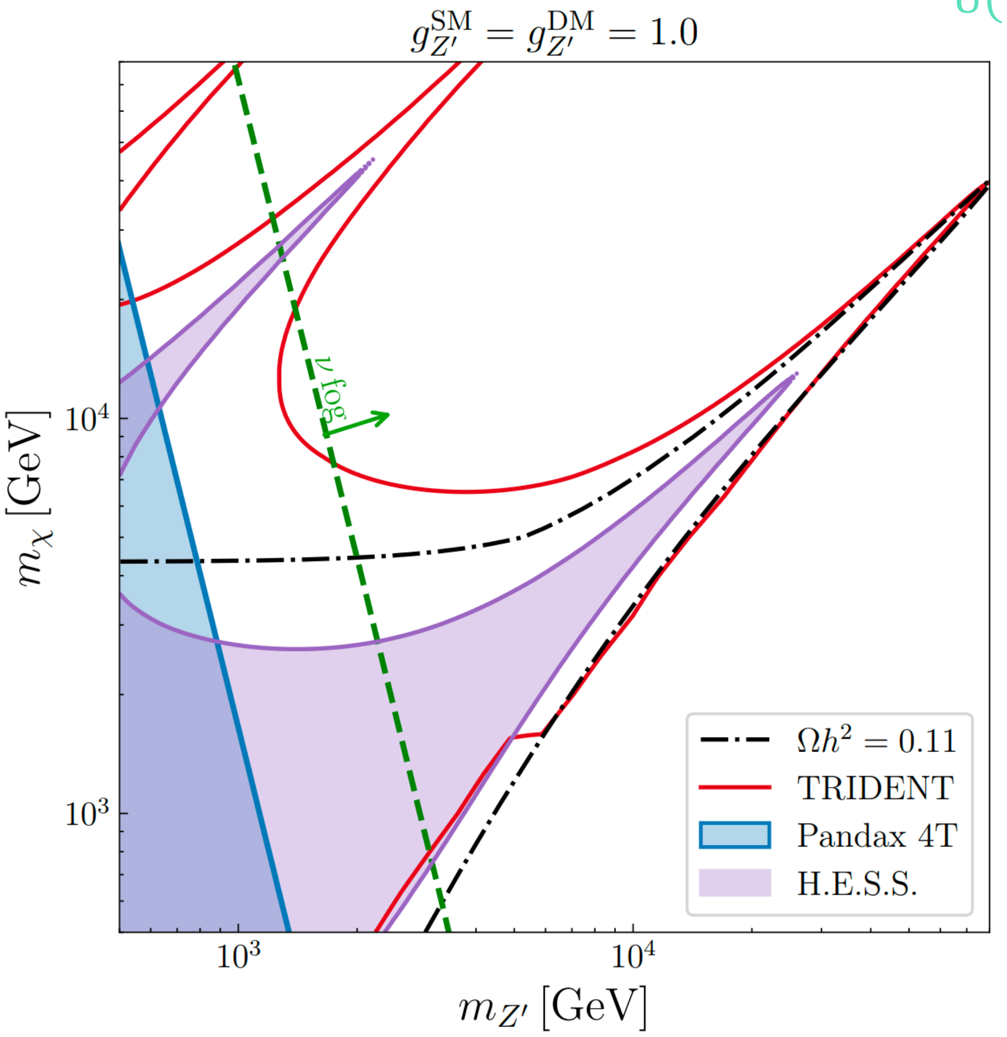

For the thermal relic and the TRIDENT constraint, the lines in the left panel of figure would be unchanged for the $L_e - L_\mu$ and $L_e - L_\tau$ models.

However, the PandaX and neutrino floor lines would move a little to the right due to a slight increase in the kinetic mixing.

For the H.E.S.S. constraint, a slight weakening of the limit would occur for the $L_e - L_\mu$ model because the e^+e^- and $\mu^+\mu^-$ final-states are less constrained.